

STING promotes proliferation and induces drug resistance via regulating the AMPK-mTOR signaling pathway in colorectal cancer cells

Huihui Yao

the First Affiliated Hospital of Soochow University

Suo Wang

Changshu Hospital Affiliated to Soochow University, First People's Hospital of Changshu City

Xin Zhou

the Second Affiliated Hospital of Soochow University

Guoqiang Zhou

Changshu No. 2 Hospital

Diyuan Zhou

the First Affiliated Hospital of Soochow University

Guoliang Chen

the First Affiliated Hospital of Soochow University

Xinyu Shi

the First Affiliated Hospital of Soochow University

Junjie Chen

the First Affiliated Hospital of Soochow University

Guanting Wu

the First Affiliated Hospital of Soochow University

Liang Sun

the First Affiliated Hospital of Soochow University

Yizhou Yao

the First Affiliated Hospital of Soochow University

Wen Gu

the First Affiliated Hospital of Soochow University

Daiwei Wan

the First Affiliated Hospital of Soochow University

Songbing He (✉ captain_hsb@163.com)

the First Affiliated Hospital of Soochow University

Keywords: Colorectal cancer, STING, Clinicopathological features, Proliferation, Drug resistance

Posted Date: March 21st, 2022

DOI: <https://doi.org/10.21203/rs.3.rs-1459358/v1>

License:  This work is licensed under a Creative Commons Attribution 4.0 International License.

[Read Full License](#)

Abstract

Background: Despite a rapidly growing body of pertinent literature, the relationship between stimulator of interferon genes (STING) protein expression and the progression of colorectal cancer (CRC) remains controversial. This study aimed to investigate the potential roles of STING as a prognostic biomarker and therapeutic target in the medical management of CRC.

Methods: STING expression was examined by immunohistochemistry to evaluate its association with clinicopathological factors. Moreover, the effects of STING on CRC cell proliferation, migration, invasiveness, and drug resistance were examined. Gene set enrichment analysis was applied to explore potential downstream mechanisms of STING in CRC. Meanwhile, we evaluated the effect of STING on glucose uptake.

Results: Our study confirmed that STING expression was significantly up-regulated in CRC tissues, and was associated with TNM stage and a poor prognosis. Additionally, STING promoted cell proliferation, migration, invasiveness, and drug resistance by mediating AMPK-mTOR signaling. Finally, we confirmed that STING regulates energy metabolism in CRC cells.

Conclusions: STING may represent a promising prognostic biomarker and therapeutic target for chemosensitization and inhibition of CRC progression.

Introduction

Colorectal cancer (CRC) is the third most common cancer worldwide. According to the newly updated GLOBOCAN 2020 estimates, CRC including anal carcinoma caused an estimated 1.9 million new cases and 935,000 deaths in 2020, ranking third in cancer incidence and second in mortality [1]. Although surgery combined with chemotherapy can substantially improve the prognosis of CRC, many patients experience poor clinical outcomes due to advanced tumor stage at the time of diagnosis, distant metastasis, and drug resistance. Exploration of the molecular mechanisms of CRC progression will facilitate the discovery of novel biomarkers and inform therapeutic strategies to improve treatment.

Stimulator of interferon genes (STING, also referred to TMEM173 and STING1), an adaptor transmembrane protein localized in the endoplasmic reticulum, is a vital innate immune sensor that detects tumor-derived DNA [2–4]. Activation of the cyclic guanosine monophosphate-adenosine 5'-monophosphate (AMP) synthase (cGAS)-STING pathway has been characterized primarily as an inflammatory mechanism in higher eukaryotes that is induced by cytosolic double-stranded DNA (dsDNA) [5]. A recent study suggests the potential roles of STING as an independent prognostic biomarker and therapeutic target to enhance anticancer immunity in CRC [6]. Although the role of the STING pathway in CRC has not been elucidated fully, multiple studies suggest that it mediates carcinogenesis [7, 8]. The rapid proliferation of cancer cells imposes a high energy demand. The AMP-activated protein kinase (AMPK)-mammalian target of the rapamycin (mTOR) pathway plays an important role in the regulation of energy metabolism. The AMPK-mTOR pathway is also related to tumor drug resistance [9, 10]. STING

is expressed in multiple human malignancies that include melanoma, gastric cancer, and hepatocellular carcinoma, and is associated with the regulation of the AMPK-mTOR pathway [10–12].

Our previous study demonstrated that fatty acid 2-hydroxylase depletion decreased the chemosensitivity of gastric cancer cells, partially because of the inhibition of AMPK and the activation of the mTOR/S6K1/Gli1 pathway [13]. GLI1 overexpression, in combination with AKT-mTOR signaling, induces drug resistance in gastric cancer [14]. However, whether STING mediates tumor regulation through the AMPK-mTOR pathway or can serve as a new therapeutic target in CRC requires further exploration. Our findings may facilitate the assessment of STING as a diagnostic biomarker and characterize the pathway by which STING regulates CRC.

Materials And Methods

Patient specimens

Thirty-two pairs of primary CRC tissues and noncancerous mucosal tissues were obtained from patients who underwent curative surgery between 2016 and 2018 at the Department of General Surgery, The First Affiliated Hospital of Soochow University (Suzhou, Jiangsu, China). Tissue specimens were stored in a liquid nitrogen tank or formalin tissue fixative immediately after resection. Clinicopathological characteristics, such as sex, age, tumor location, differentiation, growth, stage, lymphovascular invasion, and perineural invasion were obtained from the electronic medical records at the institute. The seventh edition of the American Joint Committee on Cancer guidelines for tumor, node, and metastasis (TNM) classification was used for staging. All procedures performed in this study involving human participants were in accordance with the Declaration of Helsinki (as revised in 2013). The study was approved by Biomedical Research Ethics Committee of the First Affiliated Hospital of Soochow University (Suzhou, China) (2021-NO:213), and the written informed consent was obtained from patients or their families. All clinicopathological characteristics of CRC samples are listed in Table 1.

Cell cultures and transfection

CRC cell lines (HT-29, HCT116, LoVo, SW480, and SW620) were purchased from the Cell Bank of the Chinese Academy of Sciences (Shanghai, China), which performs routine cell line authentication using single nucleotide polymorphism and short tandem repeat analyses. All cell lines were passaged for less than 4 months after resuscitation and were cultured in RPMI 1640 medium or DMEM (ThermoFisher Scientific, Carlsbad, California, USA), containing 10% FBS (Gibco), 100 U/mL penicillin G sodium, and 100 µg/mL streptomycin sulfate (Gibco) at 37 °C in a humidified atmosphere containing 5% CO₂.

For transfection. PcDNA3.1-Flag-vector and pcDNA3.1-Flag-STING plasmids encoding human wild-type (WT) STING were obtained from the Public Protein/Plasmid Library (Nanjing: China). The plasmid sequences were verified via Sanger sequencing. After being cultured at 37°C in a humidified 5% CO₂ incubator for 12 h, LoVo cells were transfected with plasmid (50 nM) using Lipofectamine 2000 (Thermo Fisher Scientific: Waltham: MA) according to the manufacturer's protocol. The plasmids were diluted with

Opti-MEM (Thermo Fisher Scientific: Waltham: MA) with the concentration of 2ug/ml for transfection and the transfected cells were cultured overnight in medium without antibiotic. Subsequent experiments were performed 24-48 h after plasmids transfection.

Protein extraction and Western blot analysis

RIPA lysis buffer (Sigma Aldrich) was used for 30 min to lyse cells to extract total protein [14]. Total protein was separated by SDS-PAGE, transferred onto a PVDF membrane, and blocked with 5% non-fat milk at room temperature for 1 h. Bands were incubated overnight with polyclonal antibodies (Cell Signaling Technology) and then with a secondary antibody bound to horseradish peroxidase (HRP) at room temperature for 2 h, and then imaged using the chemiluminescence method. Results were quantified using ImageJ software (version: 1.4.3, RRID: SCR_003070) [13].

Immunohistochemistry (IHC) and immunofluorescence staining

Paraffin-embedded tissues were cut into 5 µm sections. The sections were dewaxed twice in xylene, rehydrated with graded ethanol, and then incubated with 30% hydrogen peroxide for 10 min to block endogenous peroxidase. They were then stained with hematoxylin for 3 min and rinsed with tap water. Next, 0.5% hydrochloric acid ethanol solution was added, the sample was soaked for several seconds and then rinsed with tap water. Subsequently, the sample was stained with eosin solution for 1 min and rinsed with tap water. The samples were dehydrated with ethanol (70%, 80%, 95%, and 100%) and xylene. The tissues were sealed with neutral resin. In addition, the sections were incubated with goat serum for 30 min, then, the goat serum was removed and antibody (Cell Signaling Technology, USA, 1:200 dilution) was added at 4 °C overnight. The slides were washed with distilled water for 10 min three times and incubated with secondary antibody for 30 min. The final staining score was determined according to color intensity and positive cell rates, as described previously [13]. The score of the proportion of positive cells in the immunohistochemical sections (0, <5%, 1, 5–25%, 2, 25–50%, 3, 50–75%, 4, >75%) was multiplied by the score of staining intensity (0, negative, 1, weak, 2, moderate, 3, strong), the staining degree was then categorized into negative (0–1), weakly positive (2–3), positive (4–7), and strongly positive (8–12). In this study, immunoreactive scores of 0–4 were negative and 5–12 were positive. The IHC results were interpreted independently by two senior researchers.

Bioinformatics analysis

GSE100179 based on platform GPL17586 ([HTA-2_0] Affymetrix Human Transcriptome Array 2.0 [transcript (gene) version] contained 20 paired normal and tumor colorectal samples. We analyzed the difference of gene expression data of 40 samples. And we used “TCGA” of UALCAN (<http://ualcan.path.uab.edu/>) to analyze the correlation between the mRNA expression of STING in COAD and individual cancer stages and nodal metastasis status. Both GO and KEGG are important bioinformatics tools to annotate genes and research gene functions, biological process and signaling pathway. In our study, we analyzed these genes that interact with STING by Metascape. The PPI network for these genes was predicted using Search Tool for the Retrieval of Interacting Genes (STRING,

<https://string-db.org/>) online database. In addition, we used the "colorectal adenocarcinoma (TCGA, PanCancer Atlas)" dataset to analyze the co-expression of "STING" and "mTOR". CeRNA Network refers to the large-scale regulatory network formed between coding RNA and non-coding RNA. This hypothesis enriches our cognition of diseases and puts forward new ideas for research. At first, we successfully predicted all the miRNAs of STING using TargetScan and ENCORI. Then, we used LncBase v.2 to predict the lncRNA of these miRNAs (Pr.score>0.8). Meanwhile, we searched the expression and survival analysis of these miRNAs in COAD on ENCORI. At last, ceRNA network was constructed by Cytoscape software. In recent years, tumor regulation by immune cells has become a major topic of discussion. TIMER (Tumor Immune Estimation Resource, <https://cistrome.shinyapps.io/timer/>) made use of various immune deconvolution methods to calculate the immune infiltrates' abundances. In this work, we searched "STING, COAD" in "Gene module" and received an analysis of immune infiltration. And we showed the expression data of STING in various cancers and adjacent tissues. All gene expression data were downloaded from UCSC Xena. Then we used R-package "ggpubr" to get all the charts we need.

6-Carboxy-fluorescein phosphoramidate (FAM)-labeled siRNA (siRNA-FAM) uptake

Cells were cultured in 96-well plates for 24 h at a density of 50,000 cells/well. On the day of transfection, the cells were washed once with sterile phosphate-buffered saline (PBS), the transfection reagent (Lipofectamine™) was added into the medium RNAiMAX/liposome™ 2000) plus 5, 10, or 20 nm FAM-labeled negative control siRNA (FAM siRNA). Then, 100 µL Opti-MEM (1X), GlutaMAX, and 5% fetal bovine serum were used to replace the medium before adding the Lipofectamine RNAiMAX reagent. The reagent and different concentrations of FAM siRNA were diluted 1:1 in serum-free Opti-MEM, incubated at room temperature for 5 min, and then added to each well. After incubation at 37 °C and 5% CO₂ for 5 and 24 h, the cells were washed once with PBS. The nuclei were incubated with 1 µg/L Hoechst 33342 fluorescent DNA probe (Cell Signaling Technology) for 15 min. Images were analyzed with ImageJ software, using background subtraction.

STING silencing

SiRNA targeting human STING (specific target sequence:5'-GCAUCAAGGAUCGGGUUU-3') was synthesized by IBSBIO. A scrambled siRNA (5'-UUCUCCGAACGUGUCACGUTT-3') was used as a negative control. Cells were seeded in 6-well plates at $2.5-3 \times 10^5$ cells/well for 24 h in their respective culture medium before experiments. The STING siRNA and the negative control siRNA (both at 10 nM) were transfected using Lipofectamine RNAiMAX (Thermo Fisher Scientific) reagent for CRC cells, as described previously [13].

Cell viability

Cell viability was measured using a commercial cell counting kit-8 (Donjindo, Japan). Cells were seeded in 96-well plates at a density of 1×10^3 cells/well. After a 24 h incubation, the supernatant from each well was removed and washed twice with warm PBS. The cells in each well were added to 10 µL CCK-8 solution and 90 µL cell culture medium and incubated at 37 °C for another 2 h. Finally, the absorbance at

450 nm was measured for five consecutive days using a multifunctional microplate reader. Each procedure was performed in triplicate.

Transwell invasion and migration assay

Transwell plates (8 mm, 24-well format, Corning Incorporated, USA) were used for cell invasion and migration analysis. The matrix gel used for the invasion test was slowly thawed on ice at 4°C. The chamber insert used for invasion analysis was coated with a dilute matrix gel and dried at 37 °C. Cells (1×10^5) were suspended in 200 μ L serum-free medium and placed in the upper chamber of each incubator, 20% FBS containing complete medium was added to the lower chamber as a chemical attractant. After incubation at 37 °C for 24 h, the cells were immobilized with 4% paraformaldehyde. Finally, the transitional cells were stained with 0.3% crystal violet and quantified using a Nikon inverted microscope.

Glucose uptake assay

Cells were seeded into a 24-well plate at a density of 1×10^5 cells/well. After siRNA treatments, cells were exposed to 0.1 mM 2-NBDG (2-(N-(7-Nitrobenz-2-oxa-1, 3-diazol-4-yl) Amino)-2-Deoxyglucose) (Invitrogen, Waltham, MA, USA) in the culture medium. Plates were incubated at 37 °C with 5% CO₂ for a duration as described above. Images were obtained using identical acquisition settings on a fluorescence microscope (Leica). Mean fluorescence intensity was analyzed by Image J.

Statistical analysis

All data are presented as the mean \pm SD. Statistical analysis of the data was performed using GraphPad Prism 8.0 (GraphPad Software, Inc.). The χ^2 or Fisher's exact test was used to analyze the associations between categorical clinicopathological variables and STING expression levels. Comparisons among two experimental groups were performed using two-tailed Student's t-test. And two-way ANOVA followed by Sidak's post-hoc test was used for comparing multiple groups. $P < 0.05$ was considered to indicate a statistically significant difference.

Results

STING is upregulated in CRC and associated with advanced tumor stage and poor prognosis

Analysis of the COAD GEO dataset (GSE100179) and TCGA database, showed that the protein and mRNA expression level of STING was increased significantly in CRC tissues compared with tumor-adjacent tissues (Fig. 1A,1B). Further, as we all know, individual tumor stage and lymph node metastasis could intuitively display the condition of tumor invasion and metastasis. The outcome of UALCAN showed that the mRNA expression of STING was especially higher in patients with higher histological grade (poor differentiation) and more advanced clinical stage (Fig. 1C,1D). IHC staining disclosed STING expression in 17 of 32 tumor samples and in 4 of 32 paired adjacent tissues (Fig. 1E-1G). Furthermore, STING levels were significantly higher in cancer tissues from patients with lymphatic metastasis than in those without

lymph node metastasis (Fig. 1H, $P < 0.01$). Western blot results were similar to those of IHC staining, and indicated increased STING expression in CRC tissues compared with surrounding normal tissues (Fig. 1I-1J).

Association between STING expression and clinicopathological indicators in CRC patients

STING expression levels were classified according to IHC staining scores, and related to clinicopathological indicators. STING expression in CRC tissues was associated with lymphatic metastasis ($P < 0.05$) and TNM stage ($P < 0.05$), the STING positivity rate was significantly higher in the lymphatic metastasis and high TNM stage groups than in the no lymph node metastasis and low TNM stage groups. However, no significant associations were found among the following parameters: age, sex, tumor diameter, depth of tumor invasion, and tumor differentiation (Table 1). The P -values in each group were > 0.05 and there was no statistical difference between groups, however, statistical power may be limited by the number of samples and the effect of the cut-off value of STING expression.

Effects of targeting STING expression on proliferation, migration, invasion, and drug sensitivity of CRC cell lines

Western blotting detected STING protein expression in all five CRC cell lines. Expression levels were elevated in all CRC cell lines except LoVo, furthermore, expression levels in the HCT116 and SW480 lines were similar (Fig. 2A). Transfection of HCT116 and SW480 cells with STING-siRNA (Fig. 2B) significantly reduced STING expression (Fig. 2C). Transwell assays showed that the numbers of migrating and invading cells in the STING-KD group were significantly lower than those in the NC group (Fig. 2D-2E, $P < 0.05$). These results prove that altered STING expression can affect CRC cell migration and invasion. CCK-8 assays showed that cell proliferation in the STING-knockdown (STING-KD) group was significantly decreased compared with that of the untreated and negative control groups (NC-siRNA) at 72 h (Fig. 2F, $P < 0.05$), whereas there was no significant difference between the untreated and negative control groups. The above results suggested that elevated STING expression may promote CRC cell proliferation. Furthermore, The CCK-8 assay also showed that CRC cells in the STING-siRNA group were highly sensitive to 72 h of 5-FU exposure (Fig. 2G, $P < 0.05$).

Effects of STING on CRC cells are mediated by the AMPK-mTOR signaling pathway and STING regulates glucose uptake in CRC cells

In the present study, we conducted a series of bioinformatics analysis, including co-expression, GO, KEGG and protein-protein interaction analysis, to reveal the potential functions of STING in CRC. Firstly, construction PPI network could help us better understand the interaction between STING and other proteins. Using STRING database, we got a complex PPI network containing 21 proteins (Fig. 3A). In order to better understand the function of STING, we performed GO/KEGG enrichment analysis on 21 genes obtained from PPI network (Fig. 3B,3C). Our analysis revealed that STING was involved in regulating a series of biological processes in CRC. Meanwhile, the outcomes of cBioPortal indicated that STING is closely related to the mTOR in CRC (Fig. 3D). Combined with the above results, we put forward this

hypothesis that STING may regulate the occurrence and development of CRC through mTOR pathway. Transfection of HCT116 and SW480 cells with STING-siRNA inhibited STING expression (Fig. 3E). Meanwhile, AMPK, p-AMPK, mTOR, and p-mTOR expressions were detected (Fig. 3F). Western blot results showed that STING knockdown significantly inhibited AMPK-mTOR signaling, confirming the regulatory effect of STING. Collectively, these results suggest that STING promotes the growth and proliferation of CRC cells by inhibiting AMPK and activating the mTOR-related pathway. Based on our previous experimental results, we preliminarily proved that STING may regulate the proliferation, migration, invasiveness, and drug sensitivity of CRC cells by mediating the AMPK-mTOR pathway, which regulates a series of important functions, such as intracellular energy metabolism and biosynthesis. Firstly, AMPK and mTOR are intracellular energy receptors that balance the production, consumption, and synthesis of intracellular energy sources through negative feedback regulation to maintain homeostasis. Secondly, mTOR mediates a series of downstream signaling pathways and participates in the metabolism of sugars, lipids, amino acids, and other substances. We questioned whether the increased glucose uptake observed in tumor cells is regulated by STING signaling. Our results showed that the glucose uptake of the STING knockdown group was significantly lower than that of the control group (Fig. 3G). This suggests that STING is not only involved in regulating AMPK-mTOR pathway activity, but also regulates glucose uptake, which might further mediate CRC cell proliferation and metastasis.

hsa-miR-193b-3p may be pivotal miRNAs in ceRNA network

Based on the prediction ability of TargetScan and ENCORI, we inversely predicted the miRNA of STING. After the intersection of these miRNAs, 20 miRNAs were obtained (number of repetitions ≥ 7). Then 105 LncRNA associated with these miRNAs were predicted through LncBase v.2 (Pr. Score > 0.8). After that, we used Cytoscape to build a ceRNA network of STING (Fig. 4A,4B). After searching these 20 miRNAs on ENCORI, we found only has-miR-193b-3p could reduce the survival rate of patients and their differential expression in cancer and normal sample was notable (Fig. 4C,4D).

STING regulated the infiltration of immune cells in COAD and were key factors in a variety of tumors

The results of TIMER indicated that STING is closely related with B cell, CD4+ T cell, CD8+ T cell, Macrophage, Neutrophil and mDC cell that infiltrate the tumor tissue in COAD (Fig. 4E). Therefore, we surmised that STING influences the occurrence and development of CRC by regulating immune cell infiltration, which would be an interesting research direction. Notably, Pan-cancer analysis showed that STING was potentially a common oncogene in various cancers (Fig. 4F-4H).

Discussion

Tumorigenesis of gastrointestinal malignancies is closely related to nonspecific inflammation resulting from aberrant activation of the innate immune system [15]. Dysregulated innate immune responses mediated by STING predispose to colorectal carcinogenesis [16, 17]. STING dysfunction may cause CRC and also increase the susceptibility of melanoma cells to oncolytic viruses [16, 18], indicating that STING could represent an adjunctive therapeutic target. Furthermore, human papillomavirus E7 and adenovirus

E1A oncoproteins bind to STING and inhibit its function [19], suggesting that to some extent STING has a protective role against infections due to these oncogenic viruses. Moreover, STING expression is reduced in gastric cancer, and decreasing levels are associated with poor prognosis [20]. However, using TCGA database analysis, we found that STING expression was elevated in CRC tissues compared with normal tissues. In an earlier study, STING remained an independent prognostic biomarker of overall survival after adjusting for tumor stage and intratumoral CD8 + T-cell infiltration [6]. Furthermore, STING expression is upregulated in the consensus molecular subgroup-1 of CRC patients [5, 21]. Therefore, we speculated that elevated STING expression in CRC tissues may portend a poor prognosis. To test this hypothesis, we evaluated STING expression levels in multiple patient-derived CRC tissue specimens and corresponding adjacent normal tissues, and found that elevated STING expression in cancer tissues. In addition, we associated STING expression levels with clinical indicators, and showed that high STING expression levels were related to advanced TNM stages of CRC.

Previous studies have demonstrated that STING-mediated immune pathways are involved in the tumorigenesis of many malignancies. Abnormal STING function significantly affects, cancer cell proliferation, metastasis, and antitumor immunity. Tumor drug sensitivity is enhanced by the recruitment and infiltration of immune effector cells stimulated by STING-mediated interferon (IFN) production triggered by increased cytoplasmic dsDNA induced by adjuvant chemotherapy [17, 22–25]. However, the potential roles of STING-related pathways as therapeutic targets to inhibit tumorigenesis, enhance anti-tumor immunity, and reduce drug resistance in CRC deserve further investigation [26, 27].

In the present study, we selected HCT116 and SW480 CRC cell lines with high STING expression levels and then downregulated STING expression via siRNA interference. We then used the constructed cell model to perform relevant cell function experiments. First, we found significantly decreased CRC cell proliferation after STING knockdown, which verified the hypothesis that elevated STING expression promotes CRC cell proliferation. We also confirmed this result by using a clonogenic assay. In addition, the transwell assay indicated that STING knockdown reduced CRC cellular migration and invasiveness. Taken together, our results suggest that STING signaling significantly promotes CRC development.

STING signaling may also influence CRC drug resistance [21, 28]. Therefore, we treated CRC cells with 5-FU, and showed that proliferation of the STING-KD group was significantly lower than that of the negative control group. These results indicate that STING knockdown can improve the sensitivity of CRC cells to 5-FU. Notably, 5-FU activates the cGAS-STING pathway that produces type I IFN in CRC cells. Contrary to our results, Tian et al. reported that STING did not substantially affect the sensitivity of colon cancer cells to 5-FU *in vitro*. The authors speculated that endogenous IFN expression by cancer cells was insufficient to achieve enhanced cytotoxicity *in vitro* [28].

STING-mediated signaling also inhibits tumor growth by activating the innate immune system, thereby upregulating downstream secretion of immune regulatory factors such as IFN and the consequent recruitment and infiltration of immune effector cells that include macrophages, dendritic cells, and CD8⁺ lymphocytes [17, 18, 21]. However, functional defects in STING-related pathways may inhibit IFN

secretion in CRC cell lines [29–32]. For example, the loss of chromosome 9p carrying the IFN gene cluster is common in CRC. Tumors lacking 9p can signal through nuclear factor-kappa B downstream of STING without IFN response, which may be related to the cGAS-STING pathway [5]. However, recent study suggest that cGAS plays a unique role in protecting intestinal epithelial barrier and preventing the development of colon cancer [33]. Our study revealed that the effect of STING on CRC cells may not be mediated by the classical innate immune pathway, suggesting that STING regulates the progression of CRC and affects drug sensitivity through IFN-independent signaling.

Our study demonstrated that STING overexpression is associated with markers of advanced CRC. We constructed a STING knockdown CRC cell line and found that reduced STING expression was accompanied by decreased proliferation and migration and enhanced 5-FU sensitivity. However, STING-related signaling is often impaired in CRC. At the same time, other studies have disclosed that STING-mediated downstream antitumor immune responses activated by DNA damage enhance radiation- and chemotherapy-induced cytotoxicity [6, 25, 34]. In view of the above results, we propose that STING regulates the function of CRC cells through an IFN-independent pathway.

In this study, we first used GEO microarray data for GSEA to identify pathways that are significantly enriched after STING activation. Second, we focused on changes in mTOR-related pathway function. Combined with our previous findings [13, 14, 35], the present study demonstrates that STING activation upregulated the mTOR-related pathway. mTOR activation promotes intracellular metabolism, enhances protein synthesis, inhibits autophagy, and forms a negative feedback loop with AMPK, which plays an important role in sensing the level of intracellular nutrients and maintaining intracellular homeostasis [8]. Therefore, we suggest that STING regulates CRC cells through the AMPK-mTOR pathway. We found that AMPK function increased after STING downregulation, whereas mTOR function decreased, indicating that a series of high energy-consuming processes, such as protein synthesis and cell proliferation, was inhibited in CRC cells [36]. Meanwhile, we explored the effect of STING signaling on glucose uptake of CRC cells. The glucose uptake rate decreased with the down-regulation of STING, which confirmed that STING may regulate the energy metabolism of CRC cells. Collectively, these results suggest that the regulation of STING is mediated by the AMPK-mTOR pathway in CRC cells, which may alter energy metabolism, thereby impacting proliferation, migration, and drug sensitivity.

We have to admit that there are some limitations in our current work. We only briefly describe the effect of mTOR pathway on cell energy homeostasis. In addition, glucose entry into cells is mediated by membrane transporters. The correlation between mTOR pathway and glucose uptake seems to be very small, but it can not be ignored that mTOR pathway is closely related to autophagy. As we all know, autophagy involves a variety of organelle membranes, and the renewal of various organelle membranes is inseparable from the cell membrane. The renewal of cell membrane must involve the dynamic changes of cell membrane proteins. More importantly, there is also an important link between autophagy and energy metabolism. There is no doubt that the most important mechanism of cell metabolism is glucose metabolism. Of course, the deepening of the mechanism is also the direction of our further attention and

exploration in the future. More importantly, *in vivo* experiments and monitoring of important CRC-related indicators are warranted.

Conclusion

our results revealed a novel mechanism linking STING with the AMPK-mTOR pathway in the regulation of CRC proliferation, migration, and drug resistance, and also identified a therapeutic target to improve clinical outcomes. Notably we inversely constructed the ceRNA network of NHE family in COAD and found one critical miRNA, which could provide a basis for future research.

Declarations

Acknowledgements

Not applicable.

Authors' contributions

SH, HY, and SW conceived and designed the study and drafted the manuscript. GZ, DZ, XZ, XS, GC, JC, GW, and LS collected, analyzed, and interpreted the experimental data. YY, WG and DW revised the manuscript for important intellectual content. All authors read and approved the final manuscript.

Funding

This work was supported by National Science Foundation (NSF) of Jiangsu Province of China grants BK20191172 (S. He), Project of Key Laboratory of Clinical Pharmacy of Jiangsu Province of China XZSYSKF2020027 (G. Zhou), Project of Gusu Medical Key Talent of Suzhou City of China GSWS2020005 (S. He), Project of New Pharmaceuticals and Medical Apparatuses of Suzhou City of China SLJ2021007 (S. He) and Project of Science and Technology Development Plan of Suzhou City of China SYS2019007 (G. Zhou).

Availability of data and materials

The datasets used and/or analyzed during the current study are available from the corresponding author on reasonable request.

Ethics approval and consent to participate

This study is approved by Biomedical Research Ethics Committee of the First Affiliated Hospital of Soochow University (Suzhou, China) (2021-NO:213) and in line with the Declaration of Helsinki (as revised in 2013). Informed consent was taken from all the patients or their families.

Consent for publication

Not applicable.

Competing interests

The authors declare that they have no competing interests

References

1. Sung H, Ferlay J, Siegel RL, Laversanne M, Soerjomataram I, Jemal A, et al. Global Cancer Statistics 2020: GLOBOCAN estimates of incidence and mortality worldwide for 36 cancers in 185 countries. *CA Cancer J Clin*. 2021,71(3):209-249.
2. Ishikawa H, Ma Z, Barber GN. STING regulates intracellular DNA-mediated, type I interferon-dependent innate immunity. *Nature*. 2009,461(7265):788-92.
3. Rivera Vargas T, Benoit-Lizon I, Apetoh L. Rationale for stimulator of interferon genes-targeted cancer immunotherapy. *Eur J Cancer*. 2017, 75:86-97.
4. Corrales L, Gajewski TF. Molecular pathways: Targeting the stimulator of interferon genes (STING) in the immunotherapy of cancer. *Clin Cancer Res*. 2015, 21(21):4774-9.
5. Vashi N, Bakhom SF. The evolution of STING signaling and its involvement in cancer. *Trends Biochem Sci*. 2021,15:S0968-0004(20)30322-4.
6. Chon HJ, Kim H, Noh JH, Yang H, Lee WS, Kong SJ, et al. STING signaling is a potential immunotherapeutic target in colorectal cancer. *J Cancer*. 2019,10(20):4932-4938.
7. Marill J, Mohamed Anesary N, Paris S. DNA damage enhancement by radiotherapy-activated hafnium oxide nanoparticles improves cGAS-STING pathway activation in human colorectal cancer cells. *Radiother Oncol*. 2019,141:262-266.
8. Jiang X, Liu G, Hu Z, Chen G, Chen J, Lv Z. cGAMP inhibits tumor growth in colorectal cancer metastasis through the STING/STAT3 axis in a zebrafish xenograft model. *Fish Shellfish Immunol*. 2019,95:220-226.
9. Inoki K, Kim J, Guan KL. AMPK and mTOR in cellular energy homeostasis and drug targets. *Annu Rev Pharmacol Toxicol*. 2012,52:381-400.
10. Wang F, Alain T, Szretter KJ, Stephenson K, Pol JG, Atherton MJ, et al. S6K-STING interaction regulates cytosolic DNA-mediated activation of the transcription factor IRF3. *Nat Immunol*. 2016,17(5):514-522.
11. Prantner D, Perkins DJ, Vogel SN. AMP-activated kinase (AMPK) promotes innate immunity and antiviral defense through modulation of stimulator of interferon genes (STING) signaling. *J Biol Chem*. 2017,292(1):292-304.
12. Moretti J, Blander JM. Detection of a vita-PAMP STINGs cells into reticulophagy. *Autophagy*. 2018,14(6):1102-1104.
13. Yao Y, Yang X, Sun L, Sun S, Huang X, Zhou D, et al. Fatty acid 2-hydroxylation inhibits tumor growth and increases sensitivity to cisplatin in gastric cancer. *EBioMedicine*. 2019,41:256-267.

14. Yao Y, Zhou D, Shi D, Zhang H, Zhan S, Shao X, et al. GLI1 overexpression promotes gastric cancer cell proliferation and migration and induces drug resistance by combining with the AKT-mTOR pathway. *Biomed Pharmacother.* 2019,111:993-1004.
15. Terzić J, Grivennikov S, Karin E, Karin M. Inflammation and colon cancer. *Gastroenterology.* 2010,138(6):2101-2114.e5.
16. Xia T, Konno H, Barber GN. Recurrent loss of STING signaling in melanoma correlates with susceptibility to viral oncolysis. *Cancer Res.* 2016,76(22):6747-6759.
17. Corrales L, Glickman LH, McWhirter SM, Kanne DB, Sivick KE, Katibah GE, et al. Direct activation of STING in the tumor microenvironment leads to potent and systemic tumor regression and immunity. *Cell Rep.* 2015,11(7):1018-30.
18. Xia T, Konno H, Ahn J, Barber GN. Deregulation of STING signaling in colorectal carcinoma constrains DNA damage responses and correlates with tumorigenesis. *Cell Rep.* 2016,14(2):282-97.
19. Lau L, Gray EE, Brunette RL, Stetson DB. DNA tumor virus oncogenes antagonize the cGAS-STING DNA-sensing pathway. *Science.* 2015,350(6260):568-71.
20. Song S, Peng P, Tang Z, Zhao J, Wu W, Li H, et al. Decreased expression of STING predicts poor prognosis in patients with gastric cancer. *Sci Rep.* 2017,7:39858.
21. Chen SY, Chen S, Feng W, Li Z, Luo Y, Zhu X. A STING-related prognostic score predicts high risk patients of colorectal cancer and provides insights into immunotherapy. *Ann Transl Med.* 2021,9(1):14.
22. Woo SR, Fuentes MB, Corrales L, Spranger S, Furdyna MJ, Leung MY, et al. STING-dependent cytosolic DNA sensing mediates innate immune recognition of immunogenic tumors. *Immunity.* 2014,41(5):830-42.
23. Deng L, Liang H, Xu M, Yang X, Burnette B, Arina A, et al. STING-dependent cytosolic DNA sensing promotes radiation-induced Type I interferon-dependent antitumor immunity in immunogenic Tumors. *Immunity.* 2014,41(5):843-52.
24. Demaria O, De Gassart A, Coso S, Gestermann N, Di Domizio J, Flatz L, et al. STING activation of tumor endothelial cells initiates spontaneous and therapeutic antitumor immunity. *Proc Natl Acad Sci U S A.* 2015,112(50):15408-13.
25. Ahn J, Xia T, Konno H, Konno K, Ruiz P, Barber GN. Inflammation-driven carcinogenesis is mediated through STING. *Nat Commun.* 2014,5:5166.
26. Yi G, Brendel VP, Shu C, Li P, Palanathan S, Cheng Kao C. Single nucleotide polymorphisms of human STING can affect innate immune response to cyclic dinucleotides. *PLoS One.* 2013,8(10):e77846.
27. Cerboni S, Jeremiah N, Gentili M, Gehrman U, Conrad C, Stolzenberg MC, et al. Intrinsic antiproliferative activity of the innate sensor STING in T lymphocytes. *J Exp Med.* 2017,214(6):1769-1785.
28. Tian J, Zhang D, Kurbatov V, Wang Q, Wang Y, Fang D, et al. 5-Fluorouracil efficacy requires anti-tumor immunity triggered by cancer-cell-intrinsic STING. *EMBO J.* 2021,22:e106065.

29. Pépin G, Gantier MP. Assessing the cGAS-cGAMP-STING activity of cancer cells. *Methods Mol Biol.* 2018,1725:257-266.
30. Vander Heiden MG, DeBerardinis RJ. Understanding the intersections between metabolism and cancer biology. *Cell.* 2017,168(4):657-669.
31. Stine ZE, Walton ZE, Altman BJ, Hsieh AL, Dang CV. MYC, Metabolism, and Cancer. *Cancer Discov.*2015,5(10):1024-39.
32. Li Z, Zhang H. Reprogramming of glucose, fatty acid and amino acid metabolism for cancer progression. *Cell Mol Life Sci.* 2016,73(2):377-92.
33. Hu S, Fang Y, Chen X, Cheng T, Zhao M, Du M, et al. cGAS restricts colon cancer development by protecting intestinal barrier integrity. *Proc Natl Acad Sci U S A.* 2021,118(23):e2105747118.
34. Sprooten J, Agostinis P, Garg AD. Type I interferons and dendritic cells in cancer immunotherapy. *Int Rev Cell Mol Biol.* 2019,348:217-262.
35. Lu T, Sun L, Zhu X. Yes-associated protein enhances proliferation and attenuates sensitivity to cisplatin in human gastric cancer cells. *Biomed Pharmacother.* 2018,105:1269-1275.
36. Kim LC, Cook RS, Chen J. mTORC1 and mTORC2 in cancer and the tumor microenvironment. *Oncogene.* 2017,36(16):2191-2201.

Tables

Table 1. Association between STING and clinic-pathological factors in 32 patients with colorectal cancer.

Clinic parameters	Case No.	STING expression		P value
		None or low	High	
Total	32	15 (46.9%)	17 (53.1%)	
Age (years)				
<65	14	3 (21.4%)	11 (78.6%)	0.2656
≥65	18	8 (44.4%)	10 (55.6%)	
Gender				
Male	19	7 (36.8%)	12 (63.2%)	>0.9999
Female	13	4 (30.8%)	9 (69.2%)	
Tumor size				
≤5cm	18	7 (38.9%)	11 (61.1%)	0.7120
>5cm	14	4 (28.6%)	10 (71.4%)	
Tumor location				
Colon	12	4 (33.3%)	8 (66.7%)	>0.9999
Rectum	20	7 (35.0%)	13 (65.0%)	
Depth of invasion				
T1-2	4	2 (50.0%)	2 (50.0%)	0.5932
T3-4	28	9 (32.1%)	19 (67.9%)	
Lymph node metastasis				
Yes	21	8 (38.1%)	13 (61.9%)	0.0278*
No	11	9 (81.8%)	2 (18.2%)	
Degree of differentiation				
Well	19	7 (36.8%)	12 (63.2%)	>0.9999
Poor	13	4 (30.8%)	9 (69.2%)	
Metastasis				
Yes	8	2 (25%)	6 (75%)	0.6808
No	24	9 (37.5%)	15 (62.5%)	
Venous or Neural invasion				
Negative	21	9 (42.9%)	12 (57.1%)	0.2481

Positive	11	2 (18.2%)	9 (81.8%)	
TNM stage				
I/II	21	8 (38.1%)	13(61.9%)	0.0278*
III/IV	11	9 (81.8%)	2 (18.2%)	

* $P < 0.05$

Figures

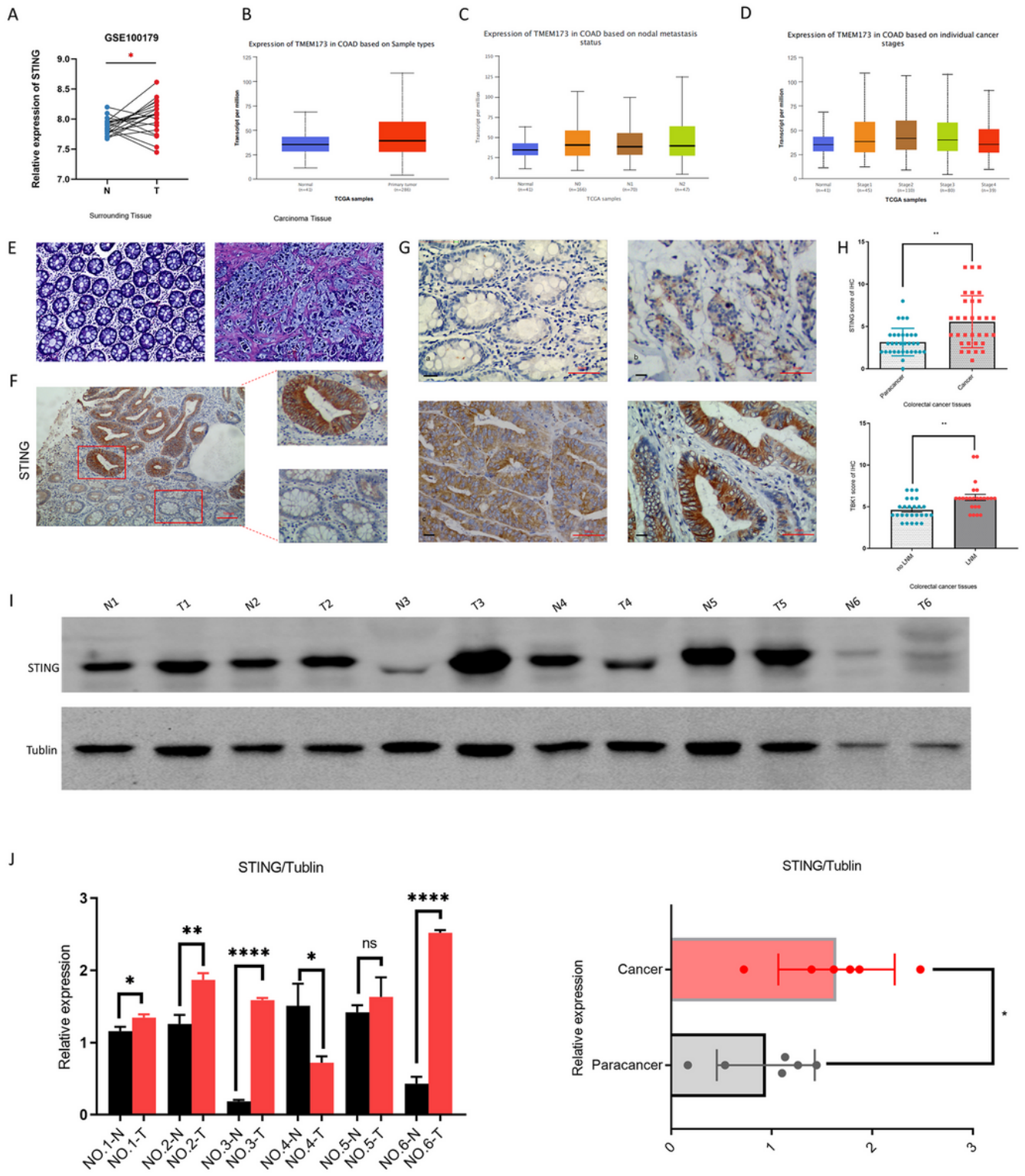


Figure 1

STING expression in colorectal cancer (CRC) and adjacent tissues.

A, B Analysis of the COAD GEO dataset (GSE100179) and TCGA database, showed that the protein and mRNA expression level of STING was increased significantly in CRC tissues compared with tumor-adjacent tissues. C, D The outcome of UALCAN showed that the mRNA expression of STING was

especially higher in patients with higher histological grade (poor differentiation) and more advanced clinical stage. E Hematoxylin-eosin staining of CRC tissue (200×, scale: 100 μm). F, G An immunohistochemical method was used to detect STING expression in 32 pairs of CRC and adjacent tissues (Fig. 1F scale: 100 μm, Fig. 1G scale: 50 μm). H IHC score of STING in 32 pairs of CRC and adjacent normal tissues: Paired samples t-test, IHC score analysis for tumor tissue with and without lymph node metastasis. I, J Western blotting was used to detect STING expression of STING in six pairs of CRC and adjacent tissues, and the gray value of cancer and adjacent tissues was analyzed quantitatively. $P < 0.05$ was considered statistically significant. Note * $P < 0.05$, ** $P < 0.01$, and *** $P < 0.001$.

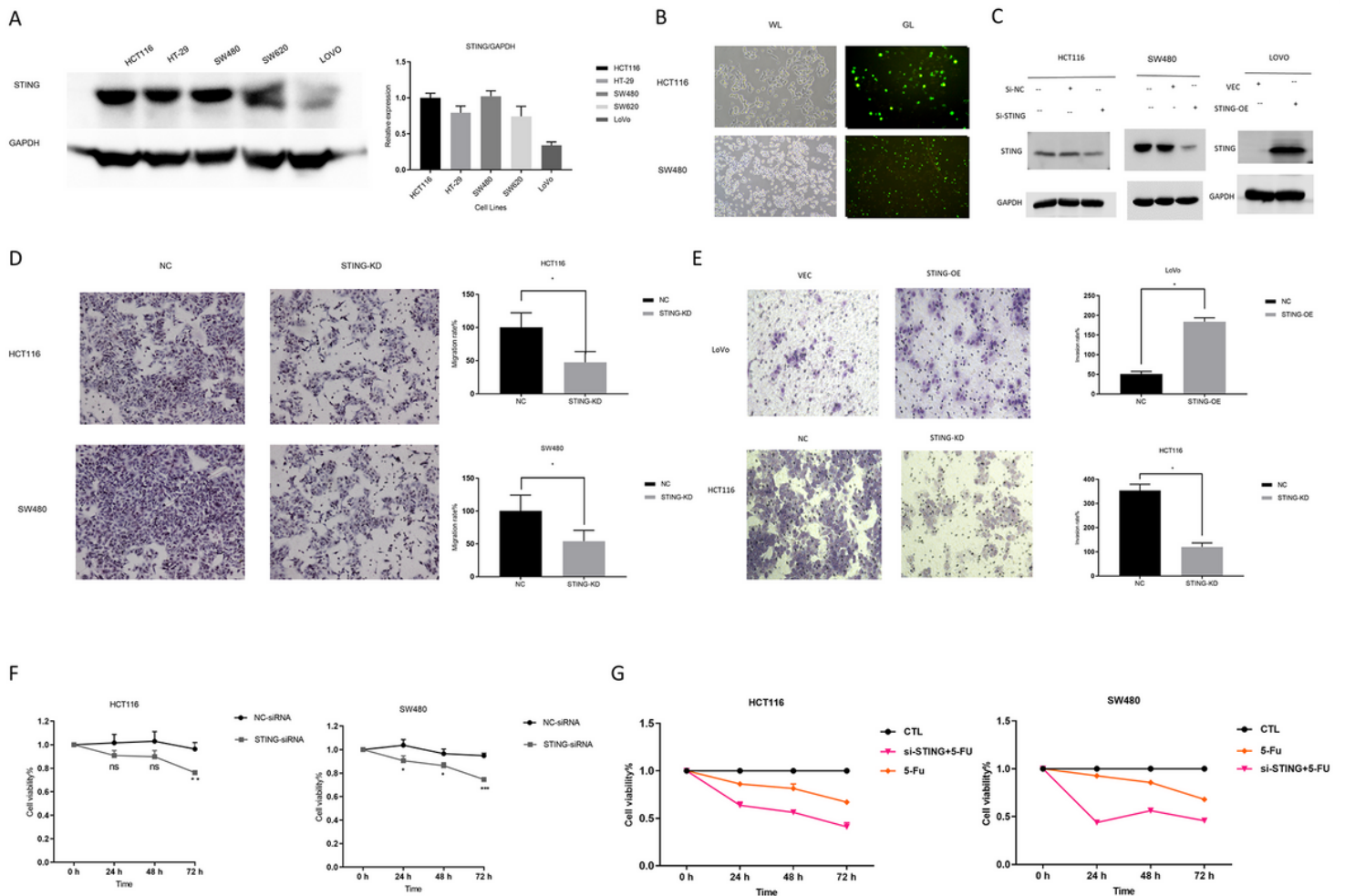


Figure 2

STING promotes CRC tumor cell growth, migration, invasiveness, and drug sensitivity. A Detection of STING expression in CRC cell lines (HCT116, HT-29, SW480, SW620, and LOVO) using western blotting, Quantitative analysis of STING expression in CRC cells. B Transfection efficiency of siRNA in CRC cells verified by fluorescent siRNA probe. C Verification of knockdown and overexpression efficiency using western blotting. D, E Twenty-four hours after transfection, numbers of migrating and invasive cells after treatment with NC-siRNA = NC and STING-siRNA = STING-KD were determined and recorded using transwell assays (three to five fields were taken for each group, and the results were analyzed

quantitatively). F The CCK-8 assay at 24, 48, and 72 h to evaluate the absorbance and proliferation of three groups of cells (NC-siRNA, and STING-siRNA). G The absorbance of concentration in each group was measured after 24, 48, and 72 h using the CCK-8 assay for the CTL group, NC-siRNA group, STING-siRNA, and 5-fluorouracil-treated cells group, respectively, and was then analyzed and calculated (5-fluorouracil concentration: 2.5 μ M). $P < 0.05$ was considered statistically significant, * $P < 0.05$.

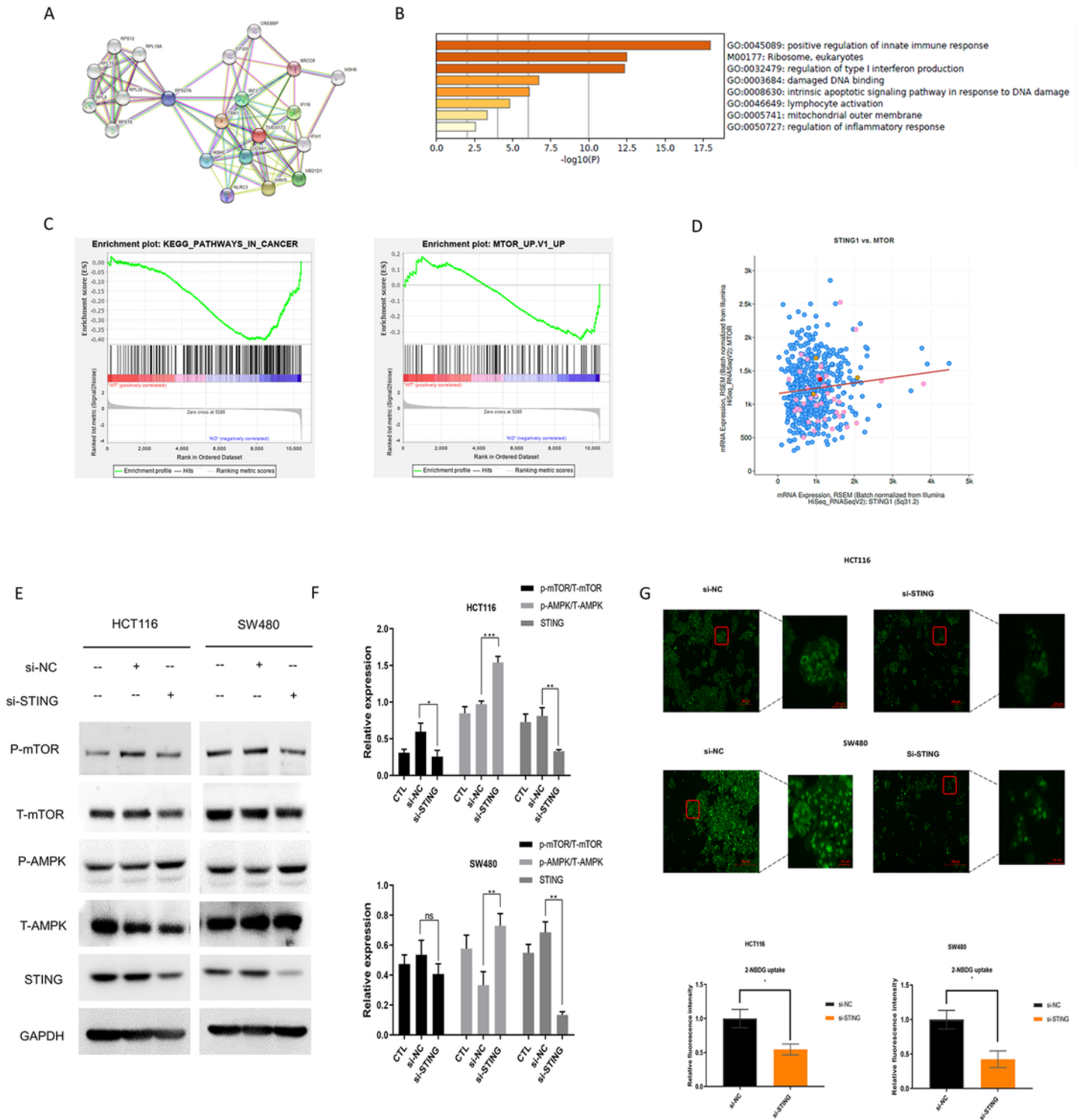


Figure 3

STING regulates biological characteristics through AMPK-mTOR pathway and glucose uptake in CRC cells. A-C GSEA using gene sequencing data from the GEO datasets GSE129436 and 100179 (KEGG enrichment, tumor-associated pathways). D cBioPortal indicated that STING is closely related to the mTOR in CRC. E STING siRNA and the negative control siRNA were transfected into HCT116 and SW480 cell lines, and the expression levels of p-mTOR, mTOR, p-AMPK, AMPK, and STING were determined by western blotting 48 h after transfection. F Quantitative analysis of the gray scale values of results from triplicates of Figure 3E. $P < 0.05$ was considered statistically significant. Note * $P < 0.05$, ** $P < 0.01$, and *** $P < 0.001$. G Glucose fluorescent probe to detect the glucose uptake of HCT116 and SW480 CRC cells. Average fluorescence intensity was quantified by randomly selecting 5 microscopic fields. (*, $P < 0.05$)

Figure 4

Bioinformatics predicted the relationship between STING and miRNA, and between STING and infiltrating immune cells. A, B ceRNA network of STING was constructed by Cytoscape. Orange oval represents mRNA, green diamond represents miRNA and blue rectangle represents LncRNA. C The expression of hsa-miR-193b-3p in COAD and normal samples from ENCORI database. D The result of overall survival for hsa-miR-149-3p in COAD from ENCORI database. E Relationship between STING expression and the infiltration of immune cells in COAD from TIMER database. F-H Pan-cancer analysis showed that STING was potentially a common oncogene in various cancers.